Rosalie Berg
Chem 415

The Low-Energy Unimolecular Reaction Rate Constants for the Gas Phase, Ni^+-Mediated Dissociation of the C−C σ Bond in Acetone

Vanessa A. Castleberry, S. Jason Dee, Otsmar J. Villarroel, Ivanna E. Laboren, Sarah E. Frey and Darrin J. Bellert*
Department of Chemistry and Biochemistry, Baylor University
J. Phys. Chem. A, 2009, 113 (39), pp 10417–10424

Introduction:

The purpose of this paper is to determine the rate constants for the unimolecular decomposition of Ni^+-$OC(CH_3)_2$ (Ni^+(Ac)), in order to better understand the processes by which metal ions catalyze the breaking of high energy bonds in organic molecules. In the past, other experimenters have studied the reactions of acetone with Iron and Cobalt ions, studying especially the thermochemistry of these reactions.

Density Functional theory has been applied to the Nickel-Acetone reaction, to determine a likely mechanism for the reaction producing ethane. This mechanism is shown in Scheme 1. According to this model, the higher energy transition state is TS_2, meaning that that rate-limiting step is the CH_3 shift.

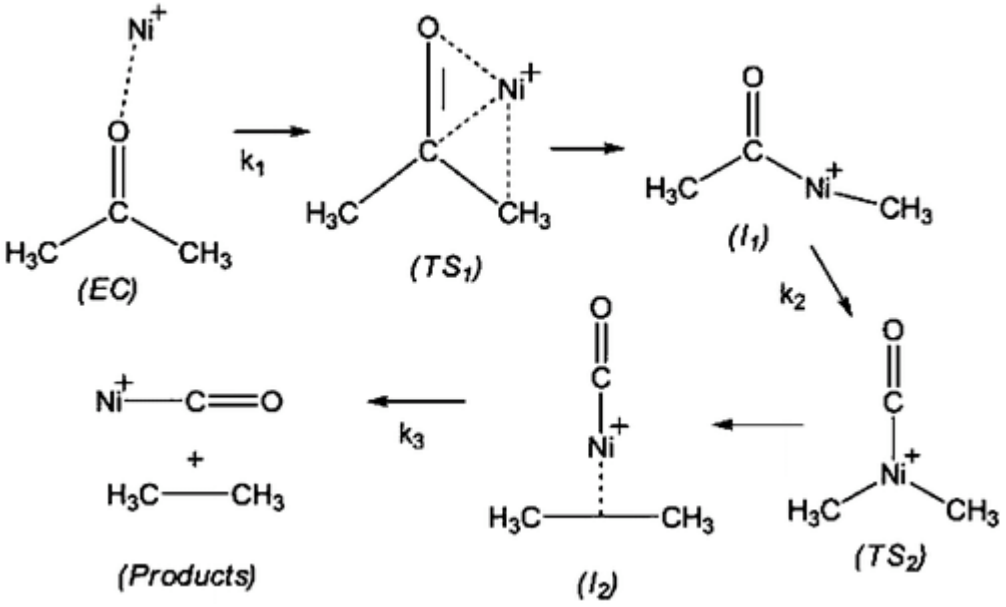

Scheme 1: Proposed mechanism of unimolecular decomposition of Ni^+(Ac)

This particular experiment uses cold precursor ions, which means that the reactants have minimal internal energy, and virtually all of the energy for the reaction is supplied by the laser photons which the molecule absorbs.

The reaction is first order and proceeds according to

$$A_t = A_0 e^{-kt} \quad (1)$$

where A_t is the amount of precursor $Ni^+(Ac)$ at time t, A_0 is the initial amount, and k is the desired rate constant. Accordingly, this experiment monitors the depletion of the $Ni^+(Ac)$ ions by way of measuring the amount of Ni^+CO fragments produced.

Experimental:

Equipment:

The general idea of the experiment is to use time of flight mass spectrometry (TOFMS) and a kinetic energy analyzer (sector) to determine the rate at which product ions are formed from the dissociating precursor ion.

High pressure Helium, doped with the vapor pressure of acetone is released in pulsed bursts into a 120 L vacuum chamber which is kept at ~3 x 10^{-6} Torr. At the end of the valve is a ¼ inch nickel rod that is constantly rotating. The nickel rod is bombarded with a pulsed laser, which vaporizes nickel atoms and ions into the helium stream. The helium stream is very cold and supersonic from the sudden expansion. The collisions between the plume of gas and the nickel particles cause the formation of cluster ions of nickel and acetone in the molecular beam.

This supersonic beam travels field free for 80cm and is skimmed twice. It then enters between the parallel capacitor plates of a Wiley-McLaren type orthogonal accelerator. This device consists of a series of parallel capacitor plates with different charges on them. Cations passing between the plates are accelerated at a right angle towards the negatively charged plate. This plate has a hole in it, through which the ions pass. There is now a third, more negative plate, and the cations are accelerated further. In the first region, particles closer to the negative plate pass through sooner, and do not accelerate as much as particles farther away. The third plate is placed to counter that effect, so that all particles leaving the accelerator appear as though they have come from a point source, with exactly the same kinetic energy.

All of the ions are accelerated at a right angle from the initial beam. The ion beam travels along a 1.8 m field free path, and enters a hemispherical kinetic energy analyzer. This device separates particles based on their kinetic energy. It allows particles of a certain kinetic energy to pass through, and it can be tuned to allow particles of different energies to pass. Beyond the kinetic energy detector is a Chevron microchannel plate detector that detects any ions that have passed through the sector, and is used to take measurements.

There is a tunable dye aimed into the oncoming supersonic beam coming out of the first vacuum chamber that can be timed to intersect the molecular beam either before it reaches the OA, or while it is in the OA. The entire assembly is shown in Figure 1.

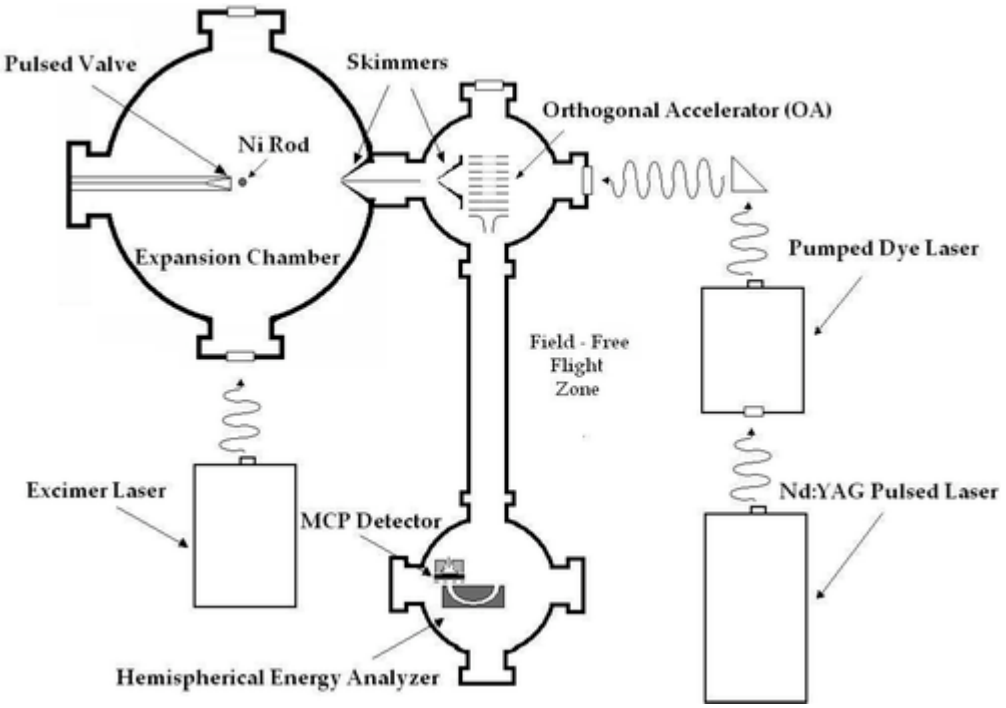

Figure 1: Diagram of instrumentation layout.

Initial experiments:

To identify the various ion clusters that are formed initially, the beam is not excited with the laser before entering the OA. All of the particles that that leave the OA have the same kinetic energy. The kinetic energy analyzer is set to that particular energy, and a mass spectrum is obtained, of the various precursor ions, shown in Figure 2.

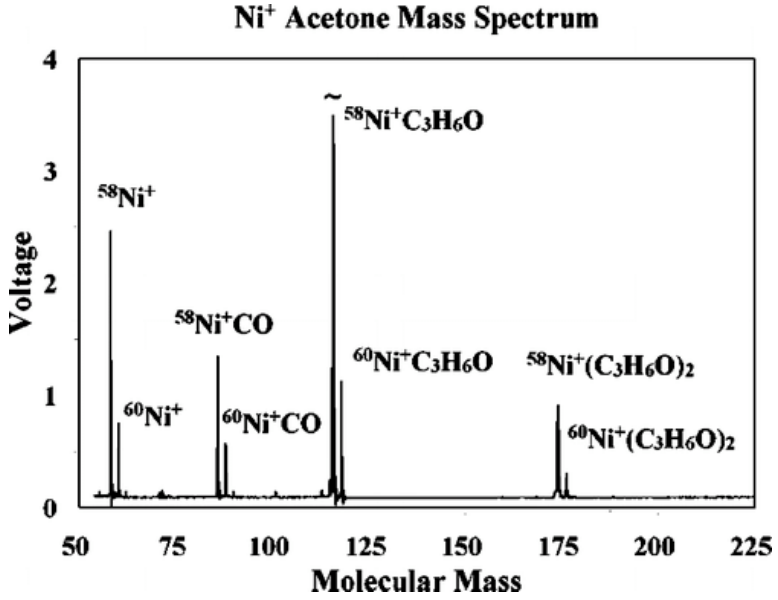

Figure 2: Time of flight mass spectrum of the various complex ions formed at the ion source.

The mass spectrum is used to determine the travel time of the desired ion cluster, $Ni^+(C_3H_6O)$. With that information, the ion beam is excited with laser 6 μs before the $Ni^+(Ac)$ ions reach the sector. The energy from the laser beam causes the cluster to undergo unimolecular decomposition. The product ions have approximately the same velocity as the precursor ion, but since they are smaller, the kinetic energy has changed. In this experiment, the voltage of the kinetic energy analyzer is varied to detect the various possible product ions of the decomposition of $Ni^+(Ac)$. The results are shown in Figure 3. The three main products observed are Ni^+, Ni^+CO, and CH_3CO^+. The peak shoulders that appear at ~365 and ~535 V are from the ^{60}Ni isotope of those clusters.

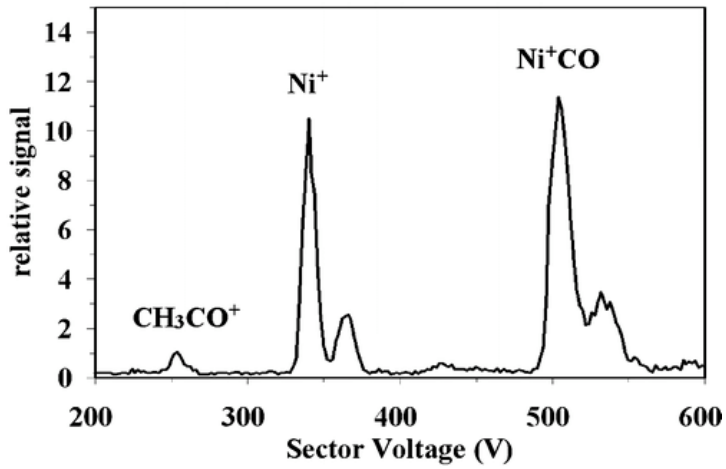

Figure 3: A scan of the dissociation product ions of $Ni^+(Ac)$

While this technique determines the possible ion fragments from the laser-induced dissociation of the precursor, the excitation occurs so close to the sector that products from both single-photon absorption, and from multiphoton absorption are detected. Only the products of single photon decomposition are desired, to better understand the kinetics. The same type of experiment, with varying sector voltage, was conducted with the excitation occurring 3 μs before the precursor ions reached the orthogonal accelerator. In theory, any multiphoton events should occur very quickly, before the beam leaves the OA. In this case, the only product ions that are detected are those that are produced after the precursor ions leave the OA, as a result of the much slower single-photon reaction. Only one peak is detected, that of Ni^+CO, indicating that that ion is the only one that is generated through single photon absorption reaction.

Main experiment:

The main purpose of the experiment is to determine the rate information for the dissociation of the $Ni^+(Ac)$ complex at various excitation energies. Laser light of various energies in the range 15600-18800 cm^{-1} intersects the at the helium/nickel/acetone beam at different amounts of time before it reaches the orthogonal accelerator. The energy excites the ion clusters, causing them to dissociate. If the cluster dissociates before it reaches the OA, then all product ions will leave the OA with the same kinetic energy as the precursor, and will not be detected by the kinetic energy analyzer. However, any dissociation events that occur during the long field free flight will result in product ions with the same velocity as the precursor and therefore different energy. The kinetic energy detector is set to allow particles to pass that have the kinetic energy of a Ni^+CO ion that has been produced by a $Ni^+(Ac)$ cluster dissociating in the field free flight path. The number of particles of this energy that travel at the velocity of $Ni^+(Ac)$ precursor ions will determine how much of the $Ni^+(Ac)$ has reacted in the field free flight path.

The laser beam intersects the molecular beam before the molecular beam reaches the orthogonal accelerator. The amount of time between laser excitation and orthogonal acceleration is varied. The amount of product ion measured for each time difference is plotted to give a decay curve – the more time between excitation and acceleration, the more ions will react before they get to the OA, and the fewer ions will be detected. This curve is fit as an exponential, and from this, the rate coefficient for the reaction (at the given level of laser excitation) is determined.

Data Analysis:

Since the unimolecular decay is a first order process, the reaction proceeds according to equation 1. However, this experiment does not directly measure the process described by equation 1. Instead, it measures the amount of precursor ions that decay after leaving the orthogonal accelerator, and before entering the kinetic energy analyzer. What is measured is the integral of equation 1, from time t_i, the time when the precursor ions leave the OA, to time t_f, the time when they enter the kinetic energy analyzer. That 'area,' (measured as the amount of Ni^+CO ions produced in that time) is plotted as y_τ versus τ, the time difference between excitation and orthogonal acceleration. When $\tau = 0$, the beam is excited while it is inside the orthogonal accelerator, nanoseconds before the OA is pulsed on. There is still a 2.4 μs delay between excitation and t_i while the ions travel through the OA. In this paper, positive τ represents earlier and earlier excitation of the molecular beam. Negative τ represents time when the OA pulses *before* the laser pulses, so that any signal observed represents a background level. (In the later paper about acetaldehyde that I presented in class, the authors reversed the meanings of positive and negative τ, perhaps to represent the chronology more directly.) The time τ equals time t_i minus the amount of time it takes to travel through the OA, (specifically, 2.4 μs).

Integrating equation 1 from t_i to t_f gives

$$y_\tau = A_0 \int_{t_i}^{t_f} e^{-kt}\,dt = \frac{A_0}{k}\left(e^{-kt_i} - e^{-k(\Delta t + t_i)}\right) = \frac{A_0}{k}\left(e^{-kt_i}\left(1 - \frac{1}{e^{k\Delta t}}\right)\right) \quad (2)$$

where $\Delta t = t_f - t_i$, which is the amount of time it takes the precursor ions to travel the field free flight zone from the OA to the kinetic energy analyzer.

Grouping the constants in equation 2 together will make equation simpler:

$$\alpha = \frac{1 - \frac{1}{e^{k\Delta t}}}{k} \quad (3)$$

Substituting equation 3 and $t_i = \tau + 2.4$ μs into equation 2 gives

$$y_\tau = \left(\frac{\alpha}{e^{2.4k}}\right) A_0 e^{-k\tau} \quad (4)$$

so plotting y_τ vs τ should yield an exponential decay curve.

Results:

Reaction Rate Constants:

Table 1 shows the rate constants for the decomposition of the $Ni^+(Ac)$ cluster ion for different laser excitation levels.

Table 1: Rate constants for the decomposition of the $Ni^+(Ac)$ cluster ion for different excitation energies.

internal energy (cm^{-1})	k(E) (s^{-1})
18800	113000□±□5000
18000	96800□±□3000
17700	92700□±□3000
16400	59000□±□2000
16100	58000□±□3000
15600	55000□±□3000

The bottom parts of Figures 4, 5, and 6 each show signal intensity (y_τ) plotted versus the delay time between excitation and orthogonal acceleration (τ). They each show exponential decay of signal with increasing time difference. The top sections each show the natural logarithm of the data in the bottom sections. The linear portion of each of the log plots was fit to a line using linear regression analysis to determine the value of k(E), the rate coefficient of the reaction at each given excitation energy. Table 1 shows a clear relationship between excitation energy and reaction rate, with more energy resulting in faster reaction rates.

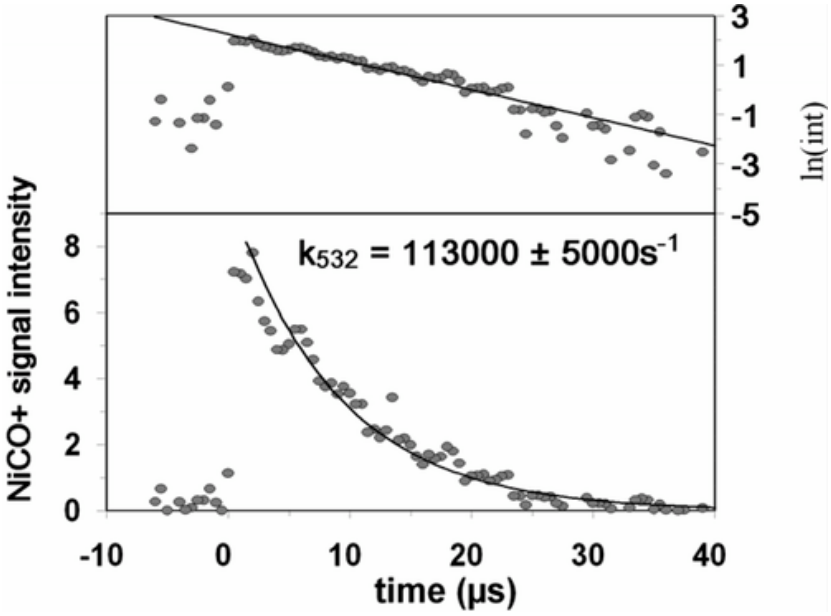

Figure 4

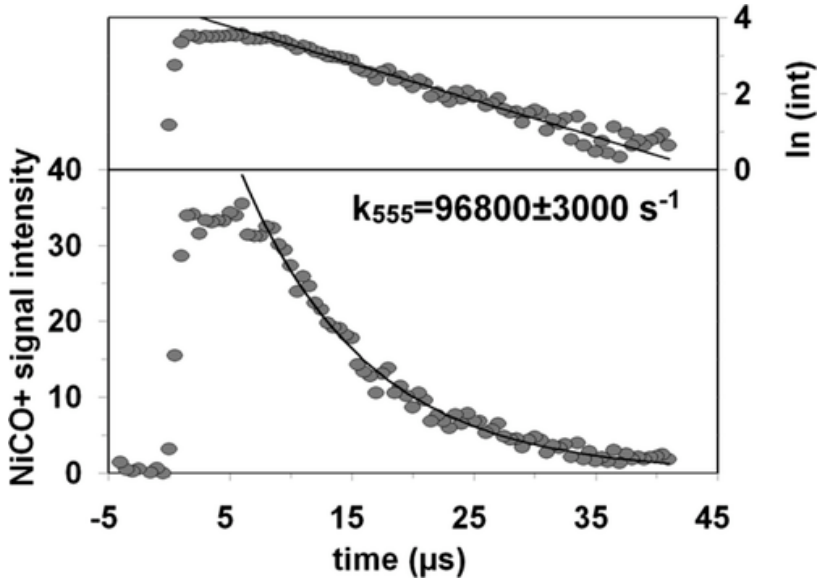

Figure 5

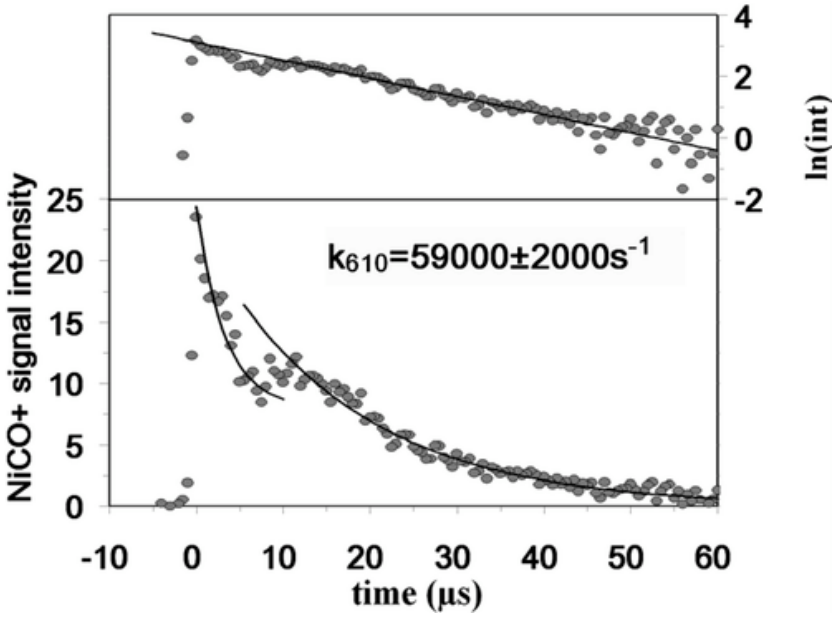

Figure 6

At different energies, the curves show slightly different behavior. Figure 4, which shows the results of the highest energy experiment, displays a curve that fits well with a single rate constant. In Figure 5, the curve shows first order decay from 8 μs onward, but before that, the data does not vary with time. Instead it takes a plateau shape. Figure 6, which shows data for an excitation level near the low end of the range of excitation energies, also has a 'delay' of 12 μs

before the exponential decay curve starts. At time differences smaller than 12 μs, there appears to be a second, very fast, reaction rate.

The mechanism given in Scheme 1 has two transition states, TS_1 and TS_2, and so it is likely that if two rate constants are measured, they each represent one of these steps of the reaction. If both steps of the reaction are kinetically important, then the relationship between product Ni^+CO ions and Ni^+Ac precursor ions can be determined

$$(Ni^+Ac)_t = (Ni^+Ac)_0 e^{-kt} \tag{5}$$

$$(I_1)_t = (Ni^+Ac)_0 \frac{k_1}{k_2 - k_1}(e^{-k_1 t} - e^{-k_2 t}) \tag{6}$$

$$(Ni^+CO)_t = \frac{(Ni^+Ac)_0}{k_2 - k_1}[k_2(1 - e^{-k_1 t}) - k_1(1 - e^{-k_2 t})] \tag{7}$$

where I_1 is intermediate 1 (I_1) from Scheme 1. The difference between the two rate constants is $\Delta k = |k_2 - k_1|$.

When Δ k is very large, equation 7 reduces to

$$(Ni^+ CO)_t = (Ni^+ Ac)_0 (1 - e^{-\kappa t}) \tag{8}$$

where κ is the larger of k_1 and k_2. In such cases, the behavior of early times of the decay curve is sharp, and the entire curve displays a single rate coefficient, κ.

When Δk is small, a time lag, called an 'induction period,' is observed between the time the precursor begins to decay, and the time the final product fragment ions are produced. The induction time is the result of either a slow initial consumption of intermediate, or else a slow initial production of intermediate. The induction times are seen in the plots of exponential decay as the time-independent features. In Figure 5, the induction time for the Ni^+Ac reaction is ~10.4 μs (8 μs from inspecting the decay curve, plus 2.4 μs travel time through the OA). In Figure 4, the induction time of the reaction is smaller than 2.4 μs, and so does not show up in the measured data.

The technique described in this paper detects only the final product of the reaction. It is therefore not possible to determine which state is the rate-limiting step without further experiments.